Article

Development and Characterization of Na$_2$CO$_3$-Activated Mozambican Bentonite: Prediction of Optimal Activation Conditions Using Statistical Design Modeling

Afonso D. Macheca [1,2,*], António B. Mapossa [3], António J. Cumbane [1], Asmina E. Sulemane [2] and Shepherd M. Tichapondwa [3]

[1] Centre of Studies in Oil and Gas Engineering and Technology, Eduardo Mondlane University, Av. de Moçambique, Km 1.5, Bairro Luís Cabral, Maputo 257, Mozambique

[2] Faculty of Engineering, Eduardo Mondlane University, Av. de Moçambique, Km 1.5, Bairro Luís Cabral, Maputo 257, Mozambique

[3] Department of Chemical Engineering, University of Pretoria, Pretoria 0002, South Africa

* Correspondence: afonso.d.macheca@uem.ac.mz

Abstract: A calcium bentonite clay from Boane region (Mozambique) was subjected to an Na$_2$CO$_3$ activation process. The methylene blue test together with energy-dispersive X-ray spectroscopy (EDX) analysis indicated the successful ion exchange of Ca^{2+} by Na$^+$ ions since the cation exchange capacity (CEC) increased from 67.5 to 74 meq/100 g and the Na/Ca ratio from 2.91 up to 15.8, as the concentration of Na$_2$CO$_3$, activation temperature, and activation time were varied from 2 to 6 wt.%, from 25 to 65 °C, and from 2 to 4 h, respectively. However, the increase in the CEC did not follow the same trend as the increase in the Na/Ca ratio, and for the case of Na$_2$CO$_3$ concentration, the increase in the CEC was limited. The X-ray diffraction (XRD) patterns also confirmed that Ca-rich bentonite was effectively modified into Na-bentonite since after the activation, the d(001) decreased from 1.52 nm to 1.30 nm. The statistical design of the experiments showed that as well as the time and the temperature × time linear interactive effect, all the other independent factors and their interactive effects had a significant influence on the CEC. The response surface methodology (RSM) indicated that higher values of the CEC can be obtained under the optimal activation conditions of 4 wt.% Na$_2$CO$_3$, at a temperature of 45 °C, and with an activation time of 3 h. A statistical model was used to predict the CEC, and the R^2 value was 0.99529, which denotes a satisfactory result in predicting the CEC.

Keywords: bentonite; clay minerals; smectite; sodium modification; cation exchange capacity

1. Introduction

Bentonite clay is one of the most widely used industrial minerals the world over. Millions of tons are utilized annually in a large variety of applications. The main traditional applications of bentonite clays include their use as drilling fluids, cements, bleaching earths, emulsions stabilizers, foundry bond clay, agricultural carriers, desiccants, pelletizing iron ores, cat box absorbents, catalysts, sealants, adhesives, cosmetics, animal feed bonds, pharmaceuticals, paints, filtering agents, paper making, environmental remediation, and construction [1,2]. Properties such as its high specific surface area, plasticity, high bonding strength, high layer charge, colloidal size and crystalline structure, and rheological and adsorptive features make bentonite an attractive product for numerous industrial applications [3–5].

Depending on the dominant exchangeable cations present in the interlamellar space, bentonite is classified as either calcium (Ca-bentonite) or sodium bentonite (Na-bentonite), each exhibiting different properties, resulting in varied applications. The terms non-swelling and swelling bentonite are synonymous with calcium and sodium bentonites [6].

Na-bentonites, however, are the most sought-after clays for most industrial applications. Their ability to absorb large amounts of water molecules and expand their dry volume many times, as well as their low permeability, results in the material exhibiting high viscosity [4,7]. The resultant thixotropic properties, higher cation exchange capacity displayed by Na-rich bentonites, and better dispersiveness in water than Ca-forms make these clays highly attractive for most engineering applications [8]. Applications in oil and gas well drilling, catalytic applications, ceramic elements, and in the production of surfactant-based organoclays for geotechnical, petroleum, and polymer nanostructured applications are just some examples of Na-bentonites' uses [9,10]. In the oil and gas well-drilling activities, for instance, Na-bentonite is the main raw material in the preparation of drilling fluids. These are viscous water-based fluids used to increase the viscosity and reduce the filtration losses of water to the surrounding rocks of the wellbore. During the well-drilling process, the water is trapped between the bentonite layers [4,11,12].

Naturally occurring Na-bentonite deposits are very rare. Sightings have been made in South Dakota, Wyoming, and Montana in the USA. The vast majority of Na-bentonites available in the world are the result of the activation processes in presence of sodium salts. Variant sodium salts can be used in the activation process; however, treatment with Na_2CO_3, also known as soda ash, is the standard and most commonly used in industrial applications [9]. The swelling capabilities and viscosity-changing properties of bentonite can be significantly improved by increasing the Na/Ca ratio. This in turn can be achieved by adding very small amounts of Na_2CO_3 to the clay, usually 2 to 4 wt.% [4,6,13–18].

Mozambique has huge reserves of bentonite. The most well-known and investigated bentonite deposit is located in the District of Boane, Maputo Province, in the South of Mozambique. Previous studies on Boane bentonite deposits indicated the presence of Ca-bentonite with about 60 wt.% montmorillonite [19–21]. According to these authors, the major problem limiting the utilization of this bentonite is the high content of impurities, with cristobalite being the major contributor, accounting for ca. 35 wt.% of the total composition. The high amount of cristobalite, which cannot be removed cost effectively, compromises the quality of the bentonite. In the work titled "Industrial Minerals of Mozambique" by Cíleck [20], it was suggested that, without any beneficiation process, Boane white bentonite was unsuitable for most industrial applications, further suggesting that the foundry industry was the only suitable destination for this clay. Given this scenario, there is a need to develop cost-effective technologies and processes to beneficiate the clay for downstream applications. Both researchers and commercial users posit that the quality of this bentonite can be improved through a chemical treatment process, even without removing the cristobalite impurity phase. The present study seeks to explore this notion.

Some work on the beneficiation of Boane white bentonite has been carried out in an attempt to upgrade its quality [19–25]. However, to the best of our knowledge, the synthesis of sodium-activated bentonite has not been reported. Therefore, this study seeks to explore the beneficiation of Boane white bentonite using a Na_2CO_3-based sodium activation process. It is hypothesized that the quality of the resultant clay will improve significantly making it attractive for use in a variety of engineering applications.

In this study, the sodium activation treatment process was carried out thermochemically and the response of the bentonite to sodium activation was assessed through CEC. Since the thermochemical sodium activation process was shown to be dependent on time, temperature, and clay chemical composition [4,26], the influence of these three factors and their interactive effects on the CEC were investigated; this was performed using a Statistical Design of Experiment approach. Finally, response surface methodology was used to optimize the activation process conditions.

2. Materials and Methods

2.1. Materials

Raw Ca-rich bentonite sample, exhibiting a white color, which occurs as a weathering product of rhyolites and rhyolitic tuffs of the Karoo volcanics distributed in the Pequenos

Libombos range [27], was obtained from Boane region, Maputo Province, Mozambique, and was supplied by Minerais Indústriais de Moçambique Lda Company (Mimoc, Maputo, Mozambique). XRF measurements (on dry basis) indicated the following chemical composition [25]: 79.5 wt.% SiO_2, 12.1 wt.% Al_2O_3, 3.44 wt.% Fe_2O_3, 0.44 wt.% CaO, 0.26 wt.% K_2O, 1.17 wt.% Na_2O, 2.87 wt.% MgO, 0.01 wt.% MnO, 0.21 wt.% TiO_2, and 0.02 wt.% P_2O_5. Methylene blue and a pure fine powder form of sodium carbonate were provided by Tecnotraguas-Mozambique and used as received.

2.2. Beneficiation of Raw Bentonite

Beneficiation of bentonite is the purification process in which the impurities are removed from raw bentonite, leaving the clay particles with a more uniform size distribution. Dry and wet sieving are the most well-known traditional methods for the purification of clays. However, wet sieving combined with sedimentation process is the most recommended one. According to Magzoub et al. [4], in the wet sieving process (using a 75 μm mesh No. 200), stable colloidal suspensions are formed when bentonite is dispersed in water (1:5 by weight) for 24 h. Any sand, quartz, feldspar, or iron impurities will not be suspended and will rapidly settle out during this process. Thus, in the present work raw bentonite samples were purified using a combined wet sieving and sedimentation process.

2.3. Sodium Carbonate Treatment

The Na_2CO_3 activation process was carried out as follow: A predetermined amount of Na_2CO_3 was first dissolved in an appropriate amount of distilled water, to produce a 4 wt.% Na_2CO_3 solution. A 6 wt.% sample of wet sieved bentonite (WSB) was dispersed in 350 mL of distilled water contained in a 500-mL glass container. The resulting clay dispersion was then mixed with the Na_2CO_3 solution and stirred using a high-speed mixer for 10 min. The activation process was performed at three different stirring times (2, 3, and 4 h), three different temperatures (25, 45, and 65 °C), and three different Na_2CO_3 concentrations (2, 4, and 6 wt.%). About 2.5% of water is expected to evaporate at the end of the stirring process. To compensate for the lost water and maintain the same bentonite concentration in the suspension, distilled water was added to the mixture [4]. After completing the activation process, the suspension was filtrated and washed with abundant distilled water to obtain bentonite cake relatively free from excess of Ca^{2+} ions. The sodium-modified samples were then dried at 60 °C in a convection oven for 24 h. Finally, the dried bentonite samples were ground into powder with an aggregate particle size of <75 μm.

2.4. Clay Sample Characterizations

The elemental composition of the clay samples was determined by x-ray fluorescense (XRF) analysis. The Thermo Fisher ARL Perform'X Sequential XRF instrument (ThermoFisher Scientific Inc., Waltham, MA, USA) with Uniquant software 5 (ThermoFisher Scientific Inc., Waltham, MA, USA) was used to collect the data. The major elemental analysis was executed on fused beads, which were obtained by milling the samples in a tungsten carbide milling pot to achieve particle sizes < 75 μm and drying them at 100 °C before roasting them at 1000 °C to determine the loss on ignition (LOI) values. One gram of sample was mixed with 6 g of lithium tetraborate flux and fused at 1050 °C to make a stable fused glass bead. X-ray diffraction (XRD) analysis was conducted on a PANalyticalX'Pert Pro powder diffractometer XRF (PANalytical, Malvern, UK) with an X'Celerator detector and variable divergence and fixed receiving slits with Fe-filtered Co-Kα radiation (λ = 1.789 Å). The mineralogy was determined by selecting the best-fitting pattern from the ICSD database to the measured diffraction pattern, using X'Pert High Score Plus software 5.1 (PANalytical, Malvern, UK). The relative phase amounts (wt.% of crystalline portion) were estimated using the Rietveld method. Thermogravimetric analysis (TGA) and thermodifferential analysis (DTA) were performed on a Perkin Elmer Pyris 4000TGA instrument (PerkinElmer, Inc., Waltham, MA, USA) using the dynamic method. About 15 mg of the sample was placed in open 150 μL alumina pans. Temperature was scanned from 25 to 950 °C at a rate

of 10 °C min^{-1} with air flowing at a rate of 50 mL min^{-1}. A Zeiss Ultra 55 FESEM Field emission scanning electron microscope (Carl Zeiss, Jena, Germany) was used to study the morphology of the clay samples at 1 kV. The clay samples were coated with carbon prior to analysis.

2.5. Determination of Cation Exchange Capacity and Na/Ca Ratio

The CEC of the original and sodium-activated bentonite samples was determined using a methylene blue test (standard test method for methylene blue index of clay, ANSI/ASTM C 837-76). The Na/Ca ratio of raw bentonites (dry and wet sieved samples) and activated samples were determined using energy-dispersive X-ray spectroscopy (EDX) conducted using a scanning electron microscopic (SEM-EDS, Jeol Instruments, Tokyo, Japan) analysis.

2.6. Statistical Design of Experiments

Factorial design is a widely-used technique when working with systems with two or more independent variables. The technique allows the testing of the effects of several factors and their interactions simultaneously [28–32]. In the present study a 2^k factorial design was used to examine the factors and their interactive effects on the CEC. Factors such as time, temperature, and Na_2CO_3 concentration were considered as the independent variables (k = 3) and CEC as the dependent variable (response). Factor levels were coded as $-$ and $+$ for the lowest and highest range of each factor used in these experiments, respectively. The study also explored the central point of each of the three factors and this was coded as 0 (Table 1). In statistical design of experiments, coded levels ($-$, 0, $+$) are represented by $X_{i,j}$.

Table 1. Coded and real levels of the factors using central composite design for CEC.

Factors	Symbol	Coded Levels		
	$-$	-1	0	$+1$
A: (Na_2CO_3), wt.%	X_1	2	4	6
B: Temperature, °C	X_2	25	45	65
C: Time, h	X_3	2	3	4

It is important to note that a 2^k factorial design assumes a linearity in the effects of the factors in the region under investigation. However, this linearity is not always a certainty. For instance, for cases where it is needed to investigate the behavior of the response at the central point of the factor, where normally the interaction terms between the factors are added, the linear model may present some torsion. For such cases, a statistical design of experiments for a 2nd order model is the most recommended. The respective classical model is represented in Equation (1).

$$Y = \beta_0 + \sum_{i=1}^{k} \beta_i X_i \sum_{i=1}^{k} \beta_{ii} X_i^2 + \sum \sum_{i<j} \beta_{ij} X_i X_j + \varepsilon \tag{1}$$

where Y is the predicted response, β_0 represents the offset term, β_i represents the linear effect, β_{ii} represents the squared effect, β_{ij} represents the interaction effect, X_i is the coded factors, and ε the error.

Statistical design of experiments for a 2nd order model can be constructed from the first order plans (2^k factorial design) by adding two experiments for each independent factor at points with $+\alpha$ and $-\alpha$ coordinates for a given factor and 0 for the remaining factors, and m_0 trials at the plan center with coordinates 0 for all coded factors. The parameter α is

called rotatability and represents the distance between a certain axial point and its central point. The value of α was calculated as follows:

$$\alpha = \left(2^k\right)^{1/4} \tag{2}$$

where k is the number of the factors.

The upper $+\alpha$ ($Z_{i,+\alpha}$) and lower $-\alpha$ ($Z_{i,-\alpha}$) levels (real levels of the variable) are determined through the Equations (3) and (4), respectively,

$$Z_{i,+\alpha} = Z_{i,0} + \alpha\Delta_i \tag{3}$$

$$Z_{i,-\alpha} = Z_{i,0} - \alpha\Delta_i \tag{4}$$

where $Z_{i,0}$ is the basic level (central level) and Δ_i is the variation range of factor, parameters calculated by the Equations (5) and (6), respectively,

$$Z_{i,0} = \frac{1}{2}(Z_{i,1} + Z_{i,2}) \tag{5}$$

$$\Delta_i = \frac{1}{2}(Z_{i,1} - Z_{i,2}) \tag{6}$$

where $Z_{i,1}$ and $Z_{i,2}$ are, respectively, the upper and lower levels (real levels) of the factors.

2.7. Prediction of Optimal Sodium Modification Conditions Using Response Surface Methodology (RSM)

In this study RSM with a central composite design was used to determine the optimal sodium modification conditions through CEC. The optimal response of the CEC that considers the relationship between the set of independent variables (Na_2CO_3 content, temperature, and time) and their interactions was predicted through Equation (1). RSM is a technique of optimization based on the use of factorial design for a specified set of factors through a mathematical models approach. The methodology, which was introduced by Box in the 1950s, uses quantitative data to evaluate the relationship of a set of controlled experimental factors and response [29–32]. Compared to the classic factorial design experiment, RSM is the most recommended as it allows a reduced number of experiments for the investigation of factor interaction, and, simultaneously, solve multivariate equations. According to Nemukula et al. [29], RSM is comprised of four important steps: (1) identification of critical factors for the process; (2) determination of the range of factor levels; (3) selection of specific test samples by the experimental design; and (4) analysis of the data by RSM and data interpretation.

Since there are 3 factors, a 2^3 standard Box–Wilson central composite design was used. The resulting design matrix contained the classic factorial design points 2^3 (1–8) augmented with 6 axial points (9–14) coded $\pm\alpha$, and 9 axial centre points (15–23), all factors at zero level. The summarized matrix of the respective combination of independent factors including the response is shown in Table 2. In this table, Z_1, Z_2, and Z_3 are the real level of the variables, with, Z_1, Z_2, and Z_3 representing the Na_2CO_3 content (wt.%), temperature (°C), and time (hours), respectively. The mathematical relationship between the real levels ($Z_{1,j}$) and coded levels ($X_{i,j}$) of the variables is given by the following equation

$$Z_{i,j} = Z_{i,0} + \Delta_i X_{i,j} \tag{7}$$

where $Z_{1,0}$ and Δ_i are calculated through Equations (5) and (6).

Using Equation (2) and considering that there are three factors in this study, the α was determined to be 1.682. Using a combination of Equations (3)–(6), the values of $Z_{i,+\alpha}$ and $Z_{i,-\alpha}$ levels were calculated (Table 3).

Table 2. Real level combinations matrix of independent variables at different levels using RSM with central composite design. CEC included in the last column is the dependent variable (response).

Run	Z_1	Z_2	Z_3
1	6	65	4
2	2	65	4
3	6	25	4
4	2	25	4
5	6	65	2
6	2	65	2
7	6	25	2
8	2	25	2
9	7.364	45	3
10	0.636	45	3
11	4	78.64	3
12	4	11.36	3
13	4	45	4.682
14	4	45	1.318
15(C)	4	45	3
16(C)	4	45	3
17(C)	4	45	3
18(C)	4	45	3
19(C)	4	45	3
20(C)	4	45	3
21(C)	4	45	3
22(C)	4	45	3
23(C)	4	45	3

(C) = Axial center points.

Table 3. Coded and real levels of the factors using central composite design for CEC applying RSM.

Factors	Coded and Real Levels				
	$-\alpha$	-1	0	$+1$	$+\alpha$
(Na_2CO_3), wt.%	0.636	2	4	6	7.364
Temperature, °C	11.36	25	45	65	78.64
Time, h	1.318	2	3	4	4.682

Statistical Analysis

The output of the experimental design was analyzed with *Statsoft Statistica* 8 software, version 8.0.360.0 English (Statsoft, Palo Alto, California, USA) and the response (CEC) was analyzed with ANOVA, coupled with the above mentioned software (*Statsoft Statistica* 8). The simultaneous interaction of the three independent factors was investigated by RSM. The model terms were selected or rejected based on the *p*-value with 95% confidence level. The quality of fit of the statistical design model was expressed by coefficient with the determination of R^2. A model validation was then carried out to investigate the adequacy of the statistical design model.

3. Results and Discussion

3.1. X-ray Fluorescence (XRF) Chemical Composition

To verify the consistency of the chemical composition of the clay under investigation, a replica of the elemental chemical analysis was carried out on the natural wet sieved sample. The XRF measurements (on dry basis) indicated the following chemical compositions: 79.6 wt.% SiO_2, 13.4 wt.% Al_2O_3, 2.52 wt.% Fe_2O_3, 0.49 wt.% CaO, 0.21 wt.% K_2O, 0.64 wt.% Na_2O, 2.97 wt.% MgO, 0.01 wt.% MnO, 0.17 wt.% TiO_2, and 0.01 wt.% P_2O_5. The high concentrations of silica and low contents of Al_2O_3 and MgO shown here when compared to typical bentonites are features that are strictly related to the parent rocks of dominantly rhyolitic composition [21,27]. The cristobalite phase present as a major impurity in the

clay is responsible for the higher content of silica [21]. The slight differences observed in the XRF analyses evident here when compared to those previously found by Malai and Macheca [25] reflect natural variations rather than composition changes caused by the processing of the samples.

3.2. X-ray Diffraction (XRD)

Figure 1 shows the X-ray diffraction (XRD) patterns (Co-Kα) of the natural wet sieved bentonite (WSB) and the selected sodium-activated sample (4.0 wt.% Na_2CO_3), showing only the most principal phases and salient peaks, namely, smectite (S) and cristobalite (C). The d-spacing of the main smectite reflection at (001) was 1.52 nm, which was in agreement with the theoretical value of the Ca^{2+}-saturated smectites [6] and consistent with the presence in the interlayer of Ca^{2+} cations embedded in the double layer of water molecules [8]. Similar results for Boane bentonite were previously reported by Cílek [20] and Muchangos [21]. This interlayer spacing suggests that this smectite contains a mixture of monovalent/divalent exchangeable cations [6]. According to these authors, under a normal relative humidity, the basal spacing d_{001} of smectite saturated with divalent exchangeable cations (Ca^{2+}, Mg^{2+}) is 1.54 nm, while for smectite saturated with monovalent exchangeable cations (Na^+) it is 1.26 nm. For smectite with a mixture of monovalent/divalent exchangeable cations, the basal spacing d_{001} is between 1.54 nm and 1.26 nm. The analysed natural Boane bentonite sample exhibited a d_{060} reflection between 0.149 nm and 0.151 nm, which is a characteristic of the dioctahedral smectite structure [33]. A similar result was previously reported by Muchangos [21]. The appearance of this peak in the treated sample allows us to conclude that the dioctahedral structure of the smectite did not undergo any changes.
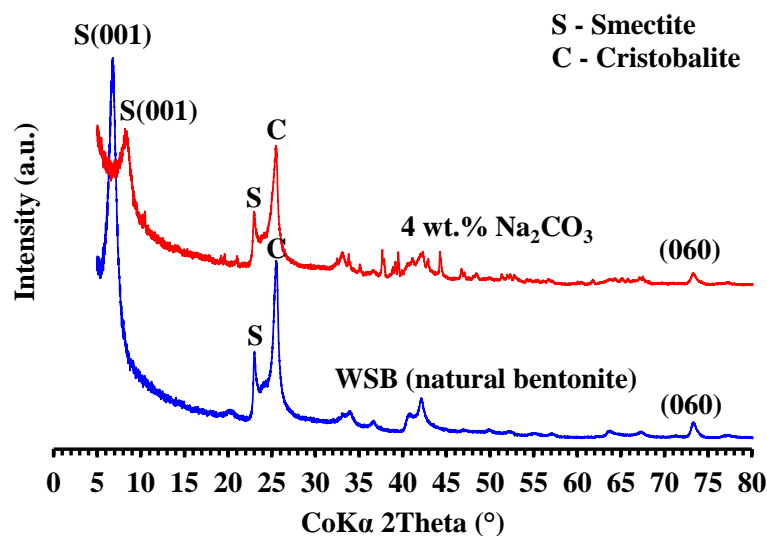

Figure 1. XRD patterns for the raw wet sieved bentonite (WSB) and 4 wt.% Na_2CO_3-modified sample.

From the figure it can be seen that the activation of bentonite with Na_2CO_3 caused structural changes in the natural bentonite, having affected mainly the (001) reflection of montmorillonite. The main smectite peak shifted to the right side, having reduced its spacing baseline from 1.52 to 1.30 nm, a value very close to the typical basal spacings of sodium montmorillonites such as the sodium form of Wyoming montmorillonite [10,34] but also characteristic of smectite with a single layer of water in the interlayer [8]. The main smectite peak of the Na_2CO_3-treated sample not only shifted to the right side but also experienced a widening and a consequent reduction in its intensity. The shift of (001) reflection to the right on the x axis and its widening suggests the displacement of Ca ions from exchange positions and the introduction of cations with the smaller atomic radius, in the specific case, Na ions. Similar results have been previously reported in the literature for Ca-montmorillonites activated with Na_2CO_3 [10,15,23,26]. However, the new peak position (1.30 nm) observed in the present study suggests that although the replacement

of Ca^{2+} cations with Na^+ occurred, the clay remains as a co-mixture of Ca-rich and Na-rich montmorillonite. This implies that in the current activation conditions used in the study, only partial cation exchange is possible. The co-existence of Ca-rich and Na-rich montmorillonite is expected when using conventional methods of bentonite activation with soda since the formation of Na-rich montmorillonite can be accompanied by the precipitation of poorly crystalline calcite or even amorphous calcium carbonate, as a result of the presence of calcium ions expelled from the interlayer [8].

From Figure 1 it can be seen that there were no changes in the characteristics of the cristobalite peak in the activated sample when compared to the natural wet sieved bentonite. This gives a clear indication that the wet sieving combined with the sedimentation process was not able to remove this impurity. This suggests that in Boane bentonite the cristobalite is finely dispersed similar to previous observations [15].

Rietveld quantitative analysis of the XRD of natural bentonite showed smectite in the form of montmorillonite as a dominant mineral phase, with about 60.6 wt.% and cristobalite with 35.1 wt.%, which is the main impurity. Other non-clay species found were quartz (3 wt.%) and calcite (2.5 wt.%). Previous XRD quantitative analysis indicated 60.3 wt.% montmorillonite, 35.7 wt.% cristobalite, and 4 wt.% quartz [19]; this sample had been purified and modified with soda ash. XRD analysis conducted by Cílek [20] on clay from the same deposit showed the following composition: montmorillonite (54 wt.%), cristobalite (35 wt.%), kaolinite (5 wt.%), calcite (3 wt.%), quartz (2 wt.%), and dolomite (1 wt.%). Bentonite samples with montmorillonite concentrations as high as 75 wt.% have been reported from other sources [21].

Commercial bentonites rarely contain less than 60% smectite and usually more than 70% [6]. Using this as a baseline, it can be concluded that Boane bentonite, with an average amount of 60 wt.% of smectite, is at the lower limit of the desirable range, and it might be considered as having a relatively high economic potential.

3.3. Thermogravimetric Analysis (TGA) and Differential Thermal Analysis (DTA)

The TGA and DTA curves of the natural wet sieved bentonite sample (WSB) and the selected sodium-activated sample (4 wt.% Na_2CO_3) are shown in Figure 2a,b. Mass loss proceeded stepwise throughout the analysed temperature range for both samples. An initial mass loss between 25 and 150 °C is observed, characteristic of smectite clays [6], with endothermic bands also being observed (see DTA curves). The endothermic bands around 72 °C for the WSB sample and 92 °C for the treated one can be attributed to the mass loss of water physically absorbed on the external surface of the clay. However, for the same range of temperatures (25 and 150 °C), the sodium-modified clay lost more mass than the natural clay. This was expected since sodium bentonites absorb more water than calcium ones.
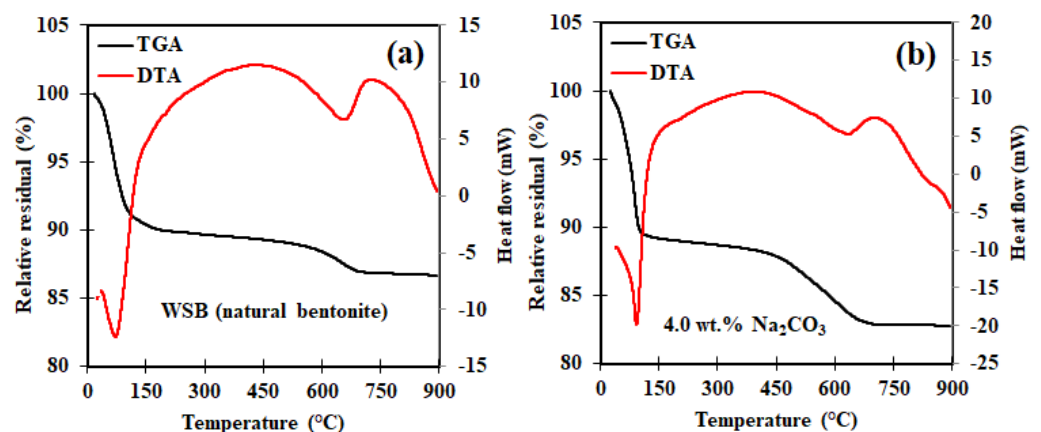

Figure 2. TGA and DTA curves for WSB (**a**) and 4 wt.% Na_2CO_3 (**b**).

The mass loss from 150 °C to about 500 °C in both samples is due to the release of the interlayer water. The occasional organic material inherently present in clay may also be released in this temperature range. In the range of approximately 500 °C and 750 °C, there was also a loss of mass with a very broad endothermic band, which is postulated to be due to aluminosilicate dehydroxylation, while the mass loss observed above 800 °C was attributed to the destruction of the crystal lattice resulting in the formation of new crystalline phases of the clay [6,8]. The most pronounced mass loss of the sodium-modified clay when compared to natural clay sample may be related to the presence of other carbonated species (carbonate minerals) such as trisodium hydrogendicarbonate dehydrate ($Na_2CO_3 \bullet NaHCO_3 \bullet 2H_2O$) and calcite ($CaCO_3$). These observations corroborate the XRD results that indicated the possible presence of poorly crystalline calcite or even amorphous calcium carbonate in the treated sample.

3.4. Scanning Electron Microscopy (SEM)

SEM images of raw dry sieved and wet sieved bentonite samples are shown in Figure 3a,b. Both micrographs exhibit similar morphologies, and therefore have some crystalline pseudo-hexagonal edges and semi rounded micro-sized particles on the surface of the clay particles. However, stacks of the dry sieved sample appeared significantly larger than those for the wet sieved sample, reaching a particle size between 20 and approximately 50 μm. In the wet sieved sample (Figure 3b), the particles appeared much looser and with a smaller size than those in the dry sieved sample. Most of the particles were much smaller than 5 μm in size. This was expected since the wet sieving process disperses the clay particles and allows pure clay to be easily separated [4].
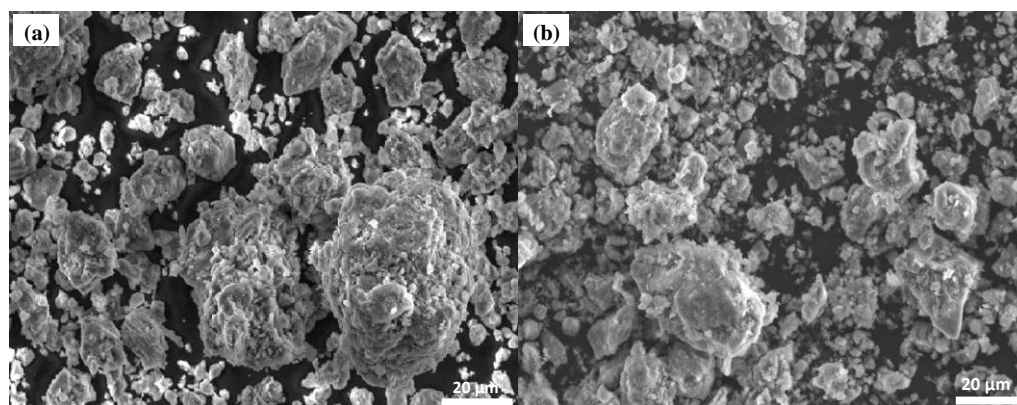

Figure 3. SEM micrographs of: (**a**) raw dry sieved and (**b**) wet sieved bentonite samples at 20 μm.

SEM micrographs of wet sieved bentonite and Na_2CO_3-modified samples, in the concentrations of 2 wt.%, 4 wt.%, and 6 wt.% Na_2CO_3 are shown in Figure 4. As can be seen in the figure, in the three treated samples, the clay particles appeared to be even looser than those in the wet sieved sample. However, the particles became larger in size, a scenario that is not surprising as the treatment process of bentonite in the presence of Na_2CO_3 leads to an increase in particle size due to their swelling [4].

3.5. Cation Exchange Capacity (CEC) Determination

The results of the CEC determined by the methylene blue test indicated a good response of the clay to the sodium treatment process in the presence of Na_2CO_3 as shown in Figure 5.
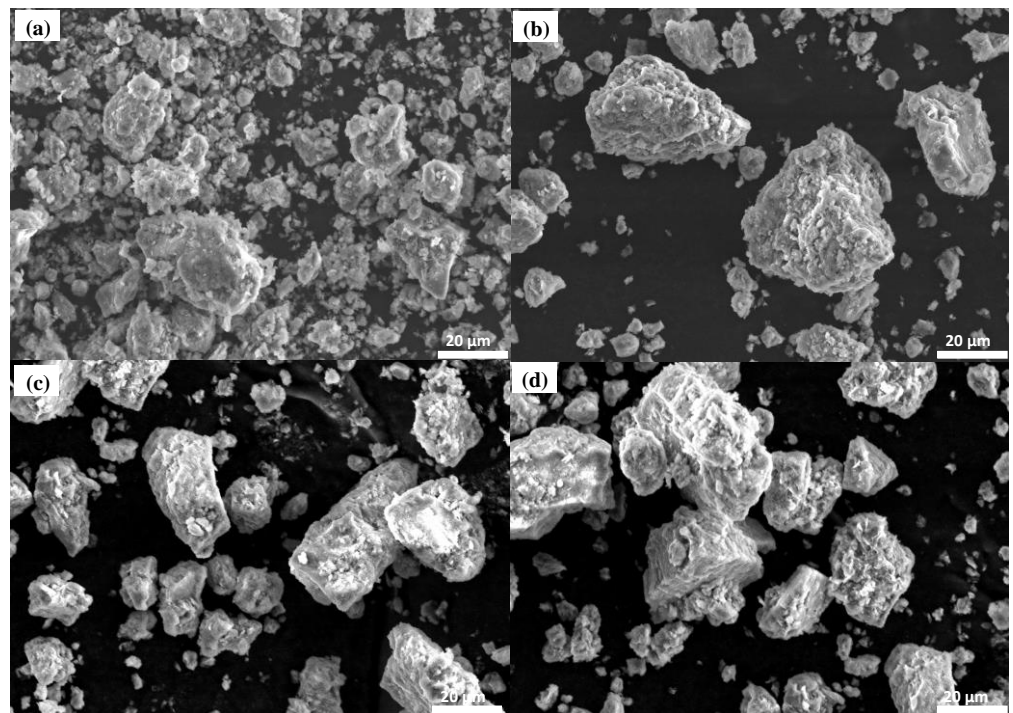
Figure 4. SEM micrographs of: (**a**) wet sieved bentonite; (**b**) 2 wt.%, (**c**) 4 wt.%, and (**d**) 6 wt.% of Na$_2$CO$_3$-modified samples. The scale bar on micrographs corresponds to 20 μm.
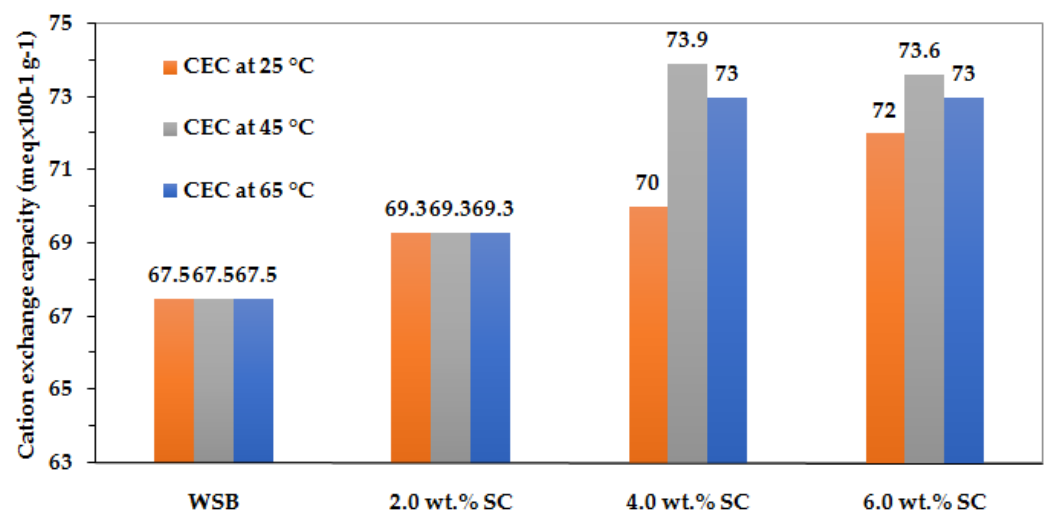

Figure 5. Effect of temperature and Na$_2$CO$_3$ concentration on CEC at fixed time (3 h). Note: WSB—wet sieved bentonite; SC—sodium carbonate.

The wet sieved neat bentonite (WSB) exhibited a CEC of about 67.5 meq/100 g, a value that lies within the range presented by typical commercial grade bentonite (40 to 120 meq/100 g) [35] and also within the range predicted by Cílek [20] for crude Boane bentonite. After activation, the CEC increased from 67.5 to as much as 74 meq/100 g as the Na$_2$CO$_3$ concentration and temperature varied from 2 to 6 wt.% and 25 to 65 °C, respectively. This indicated that the sample Ca-bentonite was effectively modified into Na-bentonite. This value (74 meq/100 g) lies within the range obtained for the so-called "relatively pure montmorillonites" (70 and 130 meq/100 g) [19].

The lower values of the CEC than expected in Boane bentonite are closely related to the high content of cristobalite, which is present at about 35 wt.% of the total composition, and other impurities such as calcite and amorphous Na$_2$CO$_3$. This is the primary reason among other existing reasons that can be pointed out. In the work titled "Industrial

Minerals of Mozambique" carried out by Cílek [20], it was suggested that for any activation process with soda ash, the CEC values would not exceed 76 meq/100 g of clay. In fact, Boane bentonite activated with soda ash on an industrial scale carried out by G&W Base and Industrial Minerals Company did not exceed 70 meq/100 g [19,23]. The CEC was determined using the methylene blue method. The fact that Boane bentonite is saturated with divalent cations, as shown by the XRD analysis, may also be behind the lower CEC values. It is well known that low CEC values of clays can be improved with the addition of inorganic matter such as soda ash or organic matter or polar organic molecules such as ethylene glycol, quaternary ammonium salts (cationic surfactants), and polyalcohols. However, because CEC is an inherent characteristic of clay, this increase is never significant. This may be one of the reasons that can explain the lower CEC values.

It is important to mention that the CEC values of the studied samples (true CEC values) may even be much greater than those reported here and the reason is simple: CEC values measured by the methylene blue method are usually lower than the so-called true "CEC", a situation which is normally attributed to the large size of the methylene blue ion and the presence of non-reactive solutes and easily soluble salts in the sample, such as chlorides and carbonates of alkali metals [6].

The results confirmed that the sodium activation process, in addition to being dependent on Na_2CO_3 concentration and temperature, was also reliant on activation time, as shown in Figure 6, similar to previous observations [4,26]. It is clear from Figures 5 and 6 that high values of CEC (74 meq/100 g) were achieved at Na_2CO_3 concentrations of 4 and 6 wt.%, temperatures of 45 and 65 °C, and with activation times of 3 and 4 h. However, for the case of Na_2CO_3 concentration, the increase in CEC is limited. At high concentrations, the CEC is practically the same and tends to decrease. In a similar work carried out by Yildiz et al. [15], a decrease in the CEC was recorded for Na_2CO_3 concentrations above 4 wt.%. The authors pointed to isomorphic substitutions as the main reason behind this situation. According to the authors, some isomorphic substitutions of the Al^{3+} by Fe^{3+} on the tetrahedral sheet and Mg^{2+} on the octahedral sheet occur on the surface of the bentonite particle. If these substitutions take place, a net negative charge develops and this charge is then balanced by adsorbed cations. If the soda ratio increases, then the net negative charge will be balanced by Na^+. Thus, the interlayer excess negative charge will decrease and the CEC will also decrease.
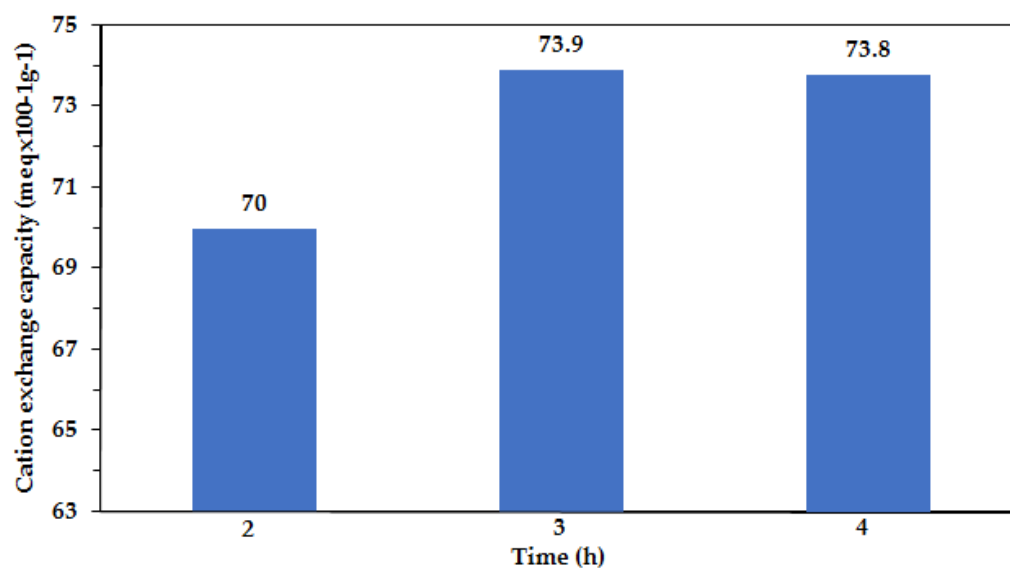

Figure 6. Effect of time on CEC at a fixed Na_2CO_3 concentration (4 wt.%) and temperature (45 °C).

3.6. Sodium/Calcium (Na/Ca) Ratio Analysis

The successful ion exchange of Ca^{2+} ions with Na^+ ions was confirmed by the results of the sodium/calcium ratios determined using energy-dispersive X-ray spectroscopy (Figure 7). The sodium and calcium contents that resulted in the ratios indicated in Figure 7 are shown in Table 4.
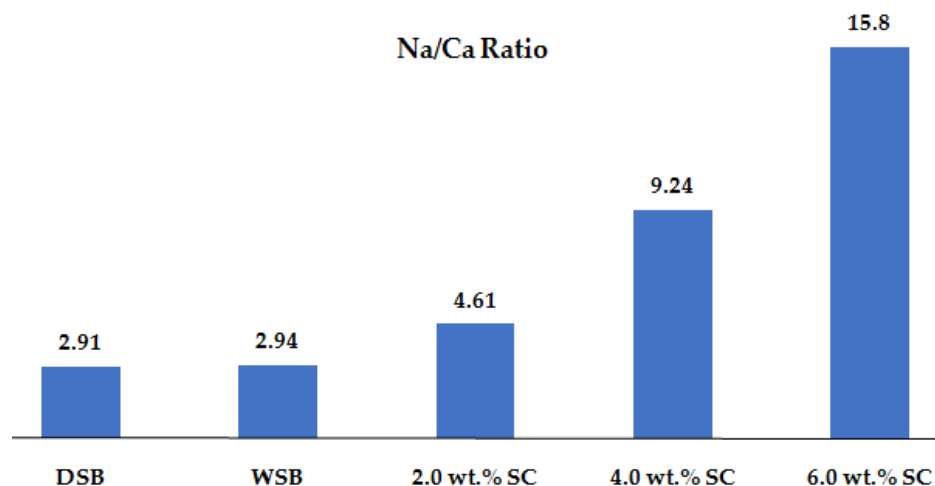

Figure 7. Na/Ca ratios for the neat clays (dried and wet sieved samples) and Na_2CO_3-activated ones. Note: WSB—wet sieved bentonite; SC—sodium carbonate.

Table 4. Sodium and calcium contents measured by EDX analysis for raw, purified, and activated bentonite samples.

Element	Sodium and Calcium Content (wt.%)				
	DSB	WSB	2.0 wt.% SC	4.0 wt.% SC	6.0 wt.% SC
Na	1.31	1.44	1.89	3.51	4.89
Ca	0.45	0.49	0.41	0.38	0.31

From Figure 7 it can be seen that the sodium/calcium ratios of raw and purified Ca-bentonite are in the range of 2.91 to 2.94. These ratios increased up to 15.8 as the concentration of Na_2CO_3 varied from 2 to 6 wt.%, similar to the previous observations reported by authors [4,7]. It is important to mention that the CEC did not increase as expected, although the Na/Ca ratio increased five times. The possible explanation for this situation is as follows: The increase in CEC does not follow the same trend as the increase in Na/Ca ratio. What is expected is that the Na/Ca ratio will grow more than the CEC for the following reasons. The CEC is a property that is closely dependent on the amount/composition of exchangeable ions present in the space between the lamellae of the clay, while the Na/Ca ratio depends not only on the exchangeable ions present in the space between the lamellae, but also on the ions present on their surface. When using energy-dispersive X-ray spectroscopy (EDX) to determine Na/Ca ratio, for example, the results will reflect the composition of both ions (from the surface and the interlayer space).

3.7. Screening of Factors for Cation Exchange Capacity

The identification of the factors and their respective interactions that are likely to affect the CEC was conducted by a factor screening experiment using the Pareto chart of the standardized effect at $p = 0.05$, as shown in Figure 8. Values > 0.05 show significant effects on the CEC [31].

Independent factors such as the Na_2CO_3 concentration, temperature, and time were considered for the factor screening experiment. The effects of the factors and their interactions on the CEC were determined according to a factorial design matrix as shown in Table 2.
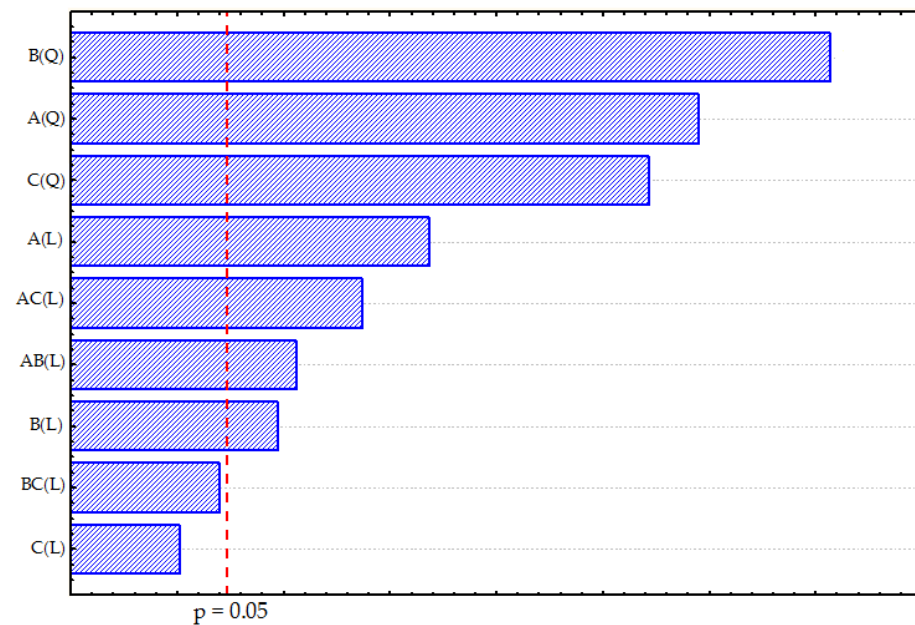
Figure 8. Pareto chart of the standardized effect for the CEC (A, Na_2CO_3 concentration; B, temperature; C, time, L, linear and Q, quadratic).

All linear and quadratic terms of the independent factors and their interactions showed significant effects on the CEC at a 95% confidence level, except for the linear term for time and the interaction term between temperature and time. The influence of the quadratic terms of the independent factors decreased in order of significance as follows: temperature > Na_2CO_3 concentration > time, while for linear terms, the Na_2CO_3 concentration had a greater significance compared to temperature. The Pareto chart further indicates that the linear stirring time factor had the least impact on the CEC of the clay.

3.8. Main Effect and Interactive Effects of the Factors

Tables 5 and 6 present the ANOVA output, and the estimated effects of the factors and the respective regression coefficients in terms of coded variables, respectively.

Table 5. ANOVA table for the CEC using central composite design.

Term	DF	SS	MS	F	*p*-Value
X_1	1	11.437	11.437	140.76	0.000
X_1^2	1	48.866	48.866	601.43	0.000
X_2	1	1.812	1.812	22.31	0.001
X_2^2	1	76.599	76.599	942.75	0.000
X_3	1	0.001	0.001	0.02	0.904
X_3^2	1	39.955	39.955	491.75	0.000
X_1X_2	1	2.531	2.531	31.15	0.001
X_1X_3	1	6.125	6.125	75.38	0.000
X_2X_3	1	0.320	0.320	3.94	0.082
Lack-of-fit	5	0.228	0.046	0.56	0.727
Pure error	8	0.650	0.081	-	-
Total	22	186.333	-	-	-

The positive signs presented by the main effects for Na_2CO_3 concentration, temperature, and time (Table 6) give a clear indication that any increase in these factors causes an increase in the CEC. However, even though the effect of time was positive, its effect on the CEC was irrelevant.

Table 6. Effect estimates and coefficients for the CEC central composite design.

Term	Effect	Coeff	SE Coeff	T	*p*-Value
Constant	73.96918	73.96918	0.094953	779.0123	0.000
X_1	1.83024	0.91512	0.077132	11.8643	0.000
X_2	0.72857	0.36428	0.077132	4.7228	0.001
X_3	0.01930	0.00965	0.077132	0.1251	0.904
X_1^2	−3.50735	−1.75368	0.071509	−24.5240	0.000
X_2^2	−4.39124	−2.19562	0.071509	−30.7043	0.000
X_3^2	−3.17148	−1.58574	0.071509	−22.1755	0.000
X_1X_2	−1.12500	−0.56250	0.100778	−5.5816	0.001
X_1X_3	−1.75000	−0.87500	0.100778	−8.6824	0.000
X_2X_3	−4.00000	−0.20000	0.100778	−1.9846	0.082
		R-Sq = 99.5% R-Sq(adj) = 99.2%			

Na_2CO_3 concentration and processing temperature are the most vital factors in the Na_2CO_3 activation of bentonites. Simultaneous heating and stirring has been shown to greatly enhance the bentonite CEC during the sodium activation processes [4,7,9].

The negative signs presented by the main effects of the quadratic terms of the factors reveal that, although statistically significant, they contribute to the reduction in the CEC. This suggests that high levels of Na_2CO_3 concentration, temperature, and time contribute to the reduction in the CEC. All interaction factors involving Na_2CO_3 concentration had significant interaction effects, except the temperature × time interactive term, which is in agreement with the Pareto chart shown in Figure 8. However, the negative signs of the effects of the interaction terms Na_2CO_3 concentration × temperature and Na_2CO_3 concentration × time indicate that, although statistically significant, the combination of these two factors contributes to the reduction in the CEC.

3.9. Optimization of the Activation Conditions

Figure 9 shows the contour plot dependency of the activation temperature and Na_2CO_3 content on the CEC generated by the *Statsoft Statistica* 8 software.
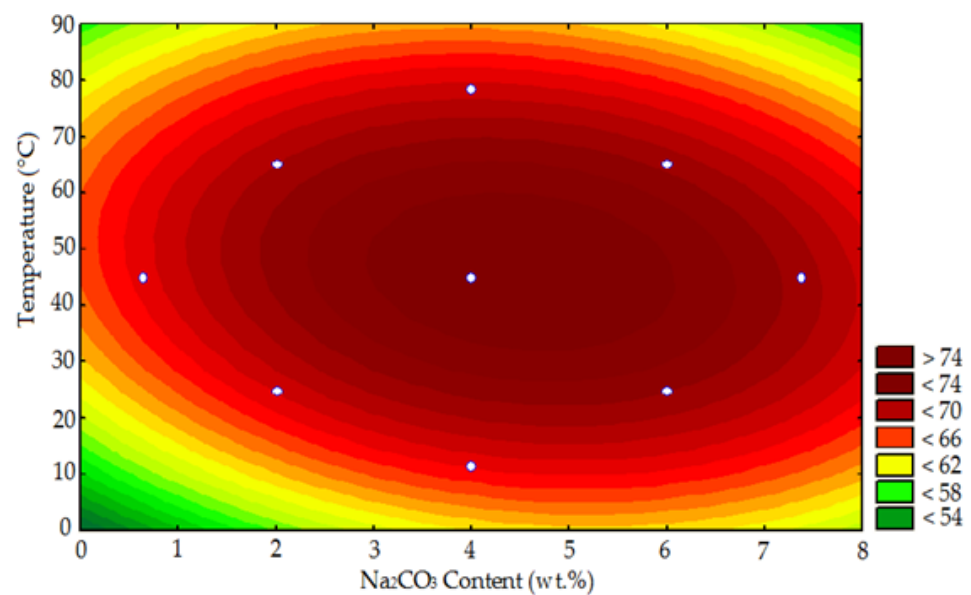

Figure 9. The contour plot dependency of activation temperature and Na_2CO_3 concentration on CEC. Note: the white points in the image represent the lower and upper limits and the central point of the factors (temperature and Na_2CO_3 concentration), including their critical points leading to a minimum and maximum CEC.

The presence of curvature allows the conclusion that the interaction effect between the Na_2CO_3 content and temperature is relevant. This somewhat corroborates the conclusions drawn in the evaluation of interaction effects made using the Pareto chart (Figure 8) and estimated effects table (Table 6). From the figure, the CEC is more sensitive to changes in temperature and Na_2CO_3 content, with more emphasis on the last parameter. This analysis can also be conducted from the estimated effects (Table 6). Table 6 confirmed that the CEC is more sensitive to changes in Na_2CO_3 content since an increase in this factor results in an increase in the CEC of almost 2% against 0.73% when compared to the increase in the activation process temperature. This fact can also be confirmed by the higher Na_2CO_3 content coefficient, which is 2.5 times greater (0.91512) than the temperature factor (0.36428). Additionally, it was observed from Figure 7, that better values of CEC could be obtained in the 3.0 to 6.0 wt.% Na_2CO_3 content range and between 30 and 60 °C. As the Na_2CO_3 content increases, Na^+ ion concentration in the liquid increases, which improves the possibility of interaction between Na^+ and Ca^{2+} and, consequently, the CEC.

The CEC passes through a maximum (74 meq/100 g). At high Na_2CO_3 concentrations, excess free Na^+ ions exist in the solution; this results in some Na^+ ions being absorbed onto the surface of the clay crystal grains leading to the formation of a hydrated shell. This in turn blocks the penetration of external moisture into the space between the crystalline layers. In this case, the ion exchange equilibrium between Na^+ and Ca^{2+} is not attained due to the high rate of ionization and activity of free Na^+ [26,36,37]. This may explain the decrease in CEC for Na_2CO_3 content above 6 wt.% as shown in Figure 9. The optimal CEC is therefore achieved with 4 wt.% Na_2CO_3 at 45 °C.

The contour plot dependency of activation time and Na_2CO_3 content on the CEC is shown in Figure 10. The curvature exhibited by the contour lines show that the effect of the interaction between these two factors contributes to the decrease in the CEC, and is significant and relevant as shown in Table 6 and Figure 8. Therefore, the CEC is more sensitive to changes in Na_2CO_3 content than time. From Table 6 it is confirmed that the CEC is more sensitive to changes in Na_2CO_3 content than time since an increase in this factor results in an increase in the CEC of almost 2% against 0.01% when compared to the increase in the activation process time. High values of CEC were obtained in the Na_2CO_3 content range between 2.5 and 7.0 wt.% and in the time range between 2 and 4.5 h. When activation time increased to 3 h, the ions' interaction was almost balanced, and the CEC was at its optimum (74 meq/100 g).
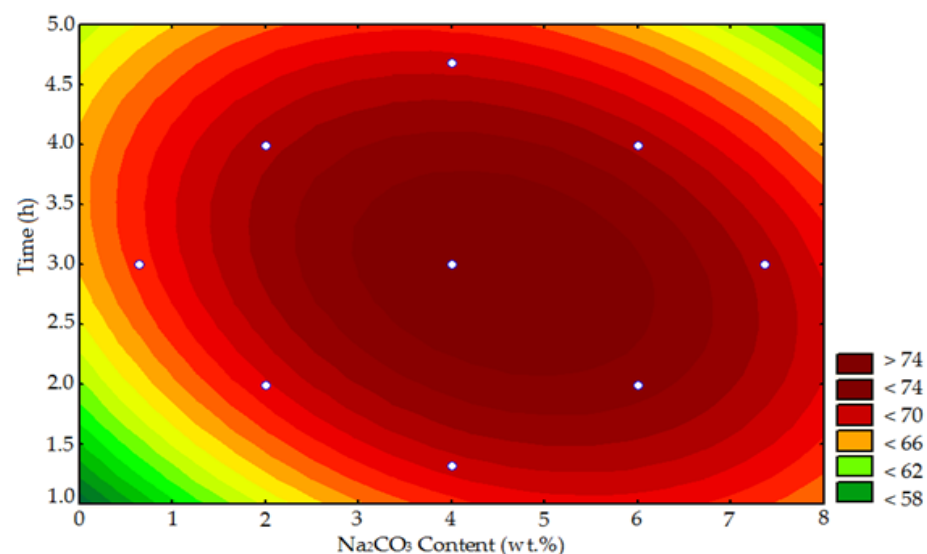

Figure 10. The contour plot dependency of stirring time and Na_2CO_3 concentration on CEC. Note: the white points in the image represent the lower and upper limits and the central point of the factors (time and Na_2CO_3 concentration), including their critical points leading to a minimum and maximum CEC.

Figure 11 shows the contour plot dependency of activation temperature and stirring time on CEC. The presence of curvature indicates that, although insignificant, the interaction of the two factors is relevant. It clearly shows that the combination of these two factors has a positive effect on the CEC as previously observed by Magzoub et al. [7]. The optimal CEC is therefore achieved at 45 °C and 3 h.
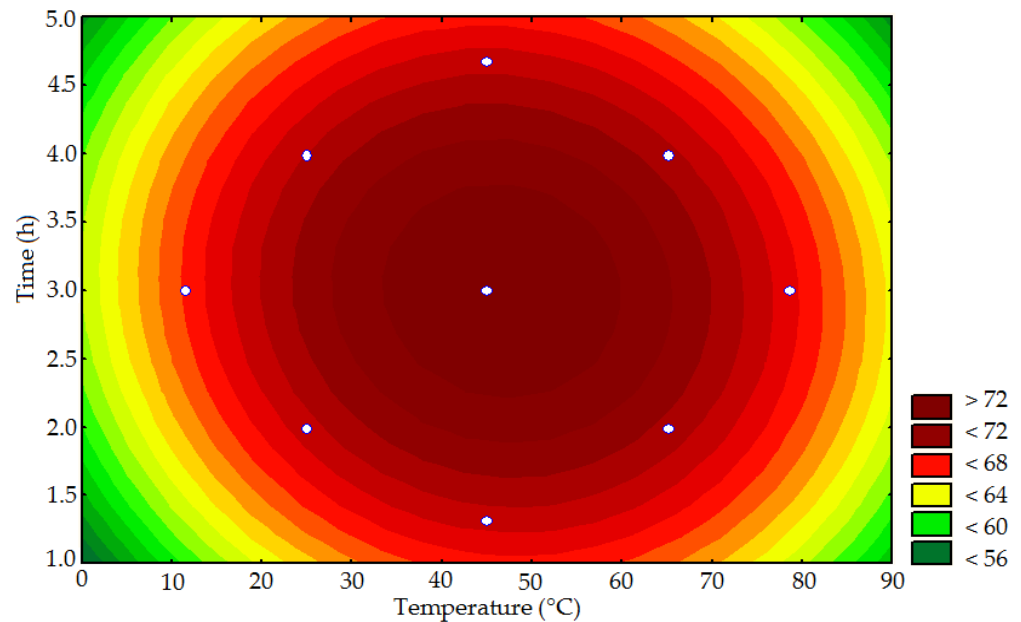

Figure 11. The contour plot dependency of activation time and temperature on CEC. Note: the white points in the image represent the lower and upper limits and the central point of the factors (time and temperature), including their critical points leading to a minimum and maximum CEC.

Critical or stationary points of the maximum CEC are shown in Table 7. The points that lead to the maximum CEC (74 meq/100 g) correspond to an Na_2CO_3 content of 4.54 wt.%, a temperature of 46.03 °C, and a time of 2.92 h, values that are within the experimental range of the investigated independent factors.

Table 7. Critical points leading to maximum CEC central composite design.

Factor	Observed Minimum	Critical Values	Observed Maximum
Z_1	0.63641	4.54273	7.36359
Z_2	11.36414	46.03231	78.63586
Z_3	1.31821	2.92492	4.68179

Figure 12 shows the normal probability plots for the CEC. Most of the checkpoints are closely distributed along the straight line, implying that the errors are distributed normally for many responses.

From the global analysis made on the results presented and discussed in Sections 3.5–3.9, it can be concluded that the sodium activation process of the white bentonite from the Boane deposit in the presence of Na_2CO_3 should be conducted using 4 wt.% Na_2CO_3 at 45 °C, and with a stirring time of 3 h. These observations agree with several researchers who have previously reported similar results [4,7,9].
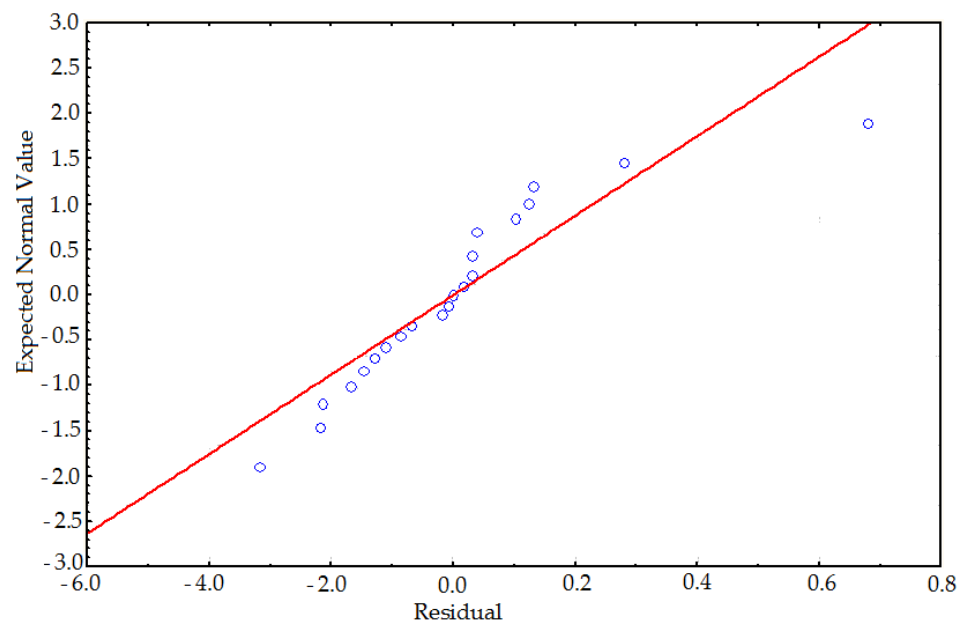
Figure 12. Normal probability plot for the CEC.

3.10. Statistical Design Model Construction

Using a statistical design of experiments for a second order model, the respective classical model (as shown in Equation (1)) can be derived. A second-order regression model was derived from the coded factors obtained from the effect estimates and coefficients for the CEC (Table 6), where only significant terms were considered for the regression model. The corresponding ANOVA was shown in Table 5. The linear terms were represented by x_1 (Na_2CO_3 content) and x_2 (temperature). The quadratic terms, x_1^2, x_2^2, and x_3^2, and interaction terms, x_1x_2 and x_1x_3, were found to be significant at a 95% confidence level. The statistical design model for the CEC in terms of coded variables (X_i) was thus constructed based on the coefficients taken from column 3 of Table 6 and their corresponding p-values (column 6), resulting in Equation (7)

$$CEC = 73.96918 + 0.91512x_1 + 0.36428x_2 - 1.75368x_1^2 - 2.19562x_2^2 - 1.58574x_3^2 - 0.56250x_1x_2 - 0.87500x_1x_3 \quad (8)$$

A similar statistical design model for the CEC in terms of the original or real variables (Z_i) was also constructed. This was performed based on the regression coefficients taken from column 2 of Table 8 and their p-values (column 4), leading to Equation (9)

$$CEC = 29.7574 + 5.9102z_1 + 0.5985z_2 + 11.7241z_3 - 0.4384z_1^2 - 0.0055z_2^2 - 1.5857z_3^2 - 0.0141z_1z_2 - 0.4375z_1z_3 \quad (9)$$

Table 8. Regression coefficients for the CEC central composite design.

Term	Reg Coefficients	T	p-Value
Constant	29.75741	23.0024	0.000
Z_1	5.91023	24.6159	0.000
Z_2	0.59848	24.3553	0.000
Z_3	11.72409	22.0748	0.000
Z_1^2	−0.43842	−24.5240	0.000
Z_2^2	−0.00549	−30.7043	0.000
Z_3^2	−1.58574	−22.1755	0.000
Z_1Z_2	−0.01406	−5.5816	0.000
Z_1Z_3	−0.43750	−8.6824	0.000
Z_2Z_3	−0.01000	−1.9846	0.082

The linear terms z_1, z_2, and z_3 represent the Na_2CO_3 content, temperature, and time, respectively, while the quadratic terms z_1^2, z_2^2, and z_3^2, and the interaction terms $z_1 z_2$ and $z_1 z_3$ used in the model were found to be significant at a 95% confidence level. The curious fact of these results is that, according to Table 8, the time factor is now statistically significant, a fact that was not verified in Table 6, which contains the regression coefficients of the coded variables. This can be explained by the fact that the original variables present values with different orders of magnitude when compared to each other [30]. Given this fact, it is recommended to analyse the significance of the coefficients using the regression coefficients of the coded variables.

A good measure of how well the model describes the experimental data that are widely used is the coefficient of determination (R^2). A perfect model will explain 100% of the variability of the experimental data. The experimental CEC vs. the predicted CEC using a statistical design model (Equation (8)) is shown in Figure 13, and the R^2 value is 0.99529, which denotes a satisfactory result in predicting the CEC.
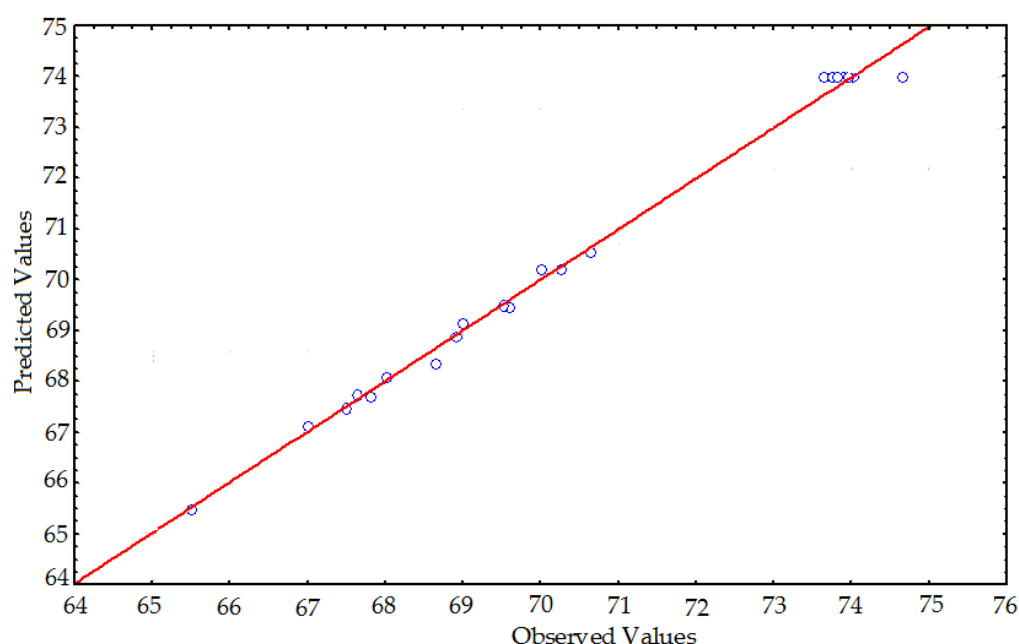

Figure 13. Predicted values vs. observed values plot for the CEC.

4. Conclusions

A calcium white-rich bentonite from Boane region (Mozambique) was thermally activated with Na_2CO_3 in an attempt to upgrade its quality. The response of the bentonite to the sodium activation process was determined through the CEC via the methylene blue method and energy-dispersive X-ray spectroscopy. Since the thermal sodium activation process is shown to be dependent on the Na_2CO_3 concentration, temperature, and activation time, the influence of these factors and their respective interactive effects on the CEC were investigated. A statistical design consisting of a factorial design and a central composite design were applied to optimize the activation process conditions. Based on the experimental results, the following conclusions were drawn.

The X-ray diffraction (XRD) patterns confirmed that Ca-rich bentonite was effectively modified into Na-bentonite since, after the activation, the d(001) decreased from 1.52 nm to 1.30 nm. The analysed Boane bentonite sample exhibited a d_{060} reflection between 0.149 nm and 0.151 nm, which is a characteristic of dioctahedral smectites.

The clay showed a good response to the sodium activation process in the presence of Na_2CO_3 since the CEC increased from 67.5 to 74 meq/100 g and the Na/Ca ratio from 2.91 up to 15.8 when the concentration of Na_2CO_3, activation temperature, and activation time

were varied from 2 to 6 wt.%, from 25 to 65 °C, and from 2 to 4 h, respectively. However, the increase in CEC did not follow the same trend as the increase in the Na/Ca ratio.

The results confirmed that the sodium activation process, in addition to being dependent on the Na_2CO_3 concentration and temperature, was also reliant on the activation time. However, for the case of Na_2CO_3 concentration, the increase in the CEC was limited. At high concentrations, the CEC was practically the same and tended to decrease. The lower values of the CEC than expected in Boane bentonite are closely related to the high content of cristobalite, which is present at about 35 wt.% of the total composition.

In the current activation conditions used in the study, only partial Ca^{2+} cation exchange is possible. The co-existence of Ca-rich and Na-rich montmorillonite was pointed out as the main reason behind this situation.

In addition to the linear term of time and the interaction term between the temperature and time effect, all independent factors and their interactive effects were shown to have a significant influence on the CEC at a 95% confidence level. For the quadratic terms of the independent factors, the decreasing order of significance was: temperature > Na_2CO_3 concentration > time, while for the linear terms, the decreasing order of significance was: Na_2CO_3 concentration > temperature. The CEC was slightly more sensitive to changes in the temperature and Na_2CO_3 concentration than in the stirring time.

The activation conditions used in the study show that the CEC passes through a maximum of about 74 meq/100 g. Higher values of the CEC can be obtained under the optimal activation conditions of 4 wt.% Na_2CO_3, at a temperature of 45 °C, and with an activation time of 3 h.

Finally, the statistical model used to predict the CEC showed a linear relationship with an R^2 value of 0.99529, which denotes a satisfactory result when compared to the observed values.

Author Contributions: Conceptualization, A.D.M.; methodology, A.D.M. and A.E.S.; software, A.D.M.; formal analysis, A.D.M., A.B.M. and A.J.C.; investigation, A.D.M., S.M.T., A.E.S. and A.B.M.; resources, A.D.M. and S.M.T.; writing—original draft preparation, A.D.M.; writing—review and editing, S.M.T. and A.B.M.; project administration, A.D.M. and A.J.C.; funding acquisition, A.D.M. and S.M.T. All authors have read and agreed to the published version of the manuscript.

Data Availability Statement: The data presented in this work are available on request from the corresponding author.

Conflicts of Interest: The authors declare no conflict of interest.

References

1. Murray, H.H. Traditional and new applications for kaolin, smectite, and palygorskite: A general overview. *Appl. Clay Sci.* **2000**, *17*, 207–221.
2. Allo, W.A.; Murray, H.H. Mineralogy, chemistry and potential applications of a white bentonite in San Juan province, Argentina. *Appl. Clay Sci.* **2004**, *25*, 237–243. [CrossRef]
3. Bergaya, F.; Lagaly, G. Surface modification of clay minerals. *Appl. Clay Sci.* **2001**, *19*, 1–3.
4. Magzoub, M.I.; Hussein, I.A.; Nasser, M.S.; Mahmoud, M.; Sultan, A.S.; Benamor, A. An investigation of the swelling kinetics of bentonite systems using particle size analysis. *J. Dispers. Sci. Technol.* **2019**, *41*, 817–827.
5. Del Hoyo, C. Layered double hydroxides and human health: An overview. *Appl. Clay Sci.* **2007**, *36*, 103–121. [CrossRef]
6. Inglethorpe, S.D.J.; Morgan, D.J.; Highley, D.E.; Bloodworth, A.J. *Industrial Minerals Laboratory Manual: Bentonite. British Geological Survey Technical Report WG/93/20*; Natural Environment Research Council: London, UK, 1993.
7. Magzoub, M.I.; Nasser, M.S.; Hussein, I.A.; Benamor, A.; Onaizi, S.A.; Sultan, A.S.; Mahmoud, M.A. Effects of sodium carbonate addition, heat and agitation on swelling and rheological behavior of Ca-bentonite colloidal dispersions. *Appl. Clay Sci.* **2017**, *147*, 176–183.
8. Bahranowski, K.; Klimek, A.; Gaweł, A.; Serwicka, E.M. Rehydration Driven Na-Activation of Bentonite—Evolution of the Clay Structure and Composition. *Materials* **2021**, *14*, 7622.

9. Karimi, L.; Salem, A. The role of bentonite particle size distribution on kinetic of cation exchange capacity. *J. Ind. Eng. Chem.* **2011**, *17*, 90–95.

10. Lazorenko, G.; Kasprzhitskii, A.; Yavna, V. Comparative study of the hydrophobicity of organo-montmorillonite modified with cationic, amphoteric and nonionic surfactants. *Minerals* **2020**, *10*, 732. [CrossRef]

11. Gidal, B.; Maly, M.; Budde, J.; Lensmeyer, G.; Pitterle, M.; Jones, J.; Caenn, R.; Chillingar, G. Drilling fluids: State of the art. *J. Pet. Sci. Eng.* **1996**, *14*, 221–230.

12. Barnes, H.A. A review of the slip (wall depletion) of polymer solutions, emulsions and particle suspensions in viscometers: Its cause, character, and cure. *J. Non-Newton. Fluid Mech.* **1995**, *56*, 221–251.

13. Lebedenko, F.; Plée, D. Some considerations on the ageing of Na_2CO_3-activated bentonites. *Appl. Clay Sci.* **1988**, *3*, 1–10.

14. Liu, D.; Edraki, M.; Berry, L. Investigating the settling behaviour of saline tailing suspensions using kaolinite, bentonite, and illite clay minerals. *Powder Technol.* **2018**, *326*, 228–236.

15. Yildiz, N.; Sarikaya, Y.; Çalimli, A. The characterization of Na_2CO_3 Activated Kütahya Bentonite. *Turk. J. Chem.* **1999**, *23*, 309–318.

16. Karagüzel, C.; Çetinel, T.; Boylu, F.; Çinku, K.; Çelik, M.S. Activation of (Na, Ca)-bentonites with soda and MgO and their utilization as drilling mud. *Appl. Clay Sci.* **2010**, *48*, 398–404.

17. Brandenburg, U.; Lagaly, G. Rheological properties of sodium montmorillonite dispersions. *Appl. Clay Sci.* **1988**, *3*, 263–279.

18. Singh, P.K.; Sharma, V.P. Effect of additives and aging on the rheological properties of water-based drilling fluid. *Energy Sources* **1991**, *13*, 369–387.

19. Massinga, P.H., Jr.; Focke, W.W.; De Vaal, P.L.; Atanasova, M. Alkyl ammonium intercalation of Mozambican bentonite. *Appl. Clay Sci.* **2010**, *49*, 142–148. [CrossRef]

20. Cílek, V. *Industrial Minerals of Mozambique*, 1st ed.; Czech Geological Office: Prague, Czech Republic, 1989; pp. 143–149.

21. Muchangos, A.C.D. Mineralogy and Geochemistry of Bauxite and Bentonite Deposits from Mozambique. Doctoral Thesis, Utrecht University, Utrecht, The Netherlands, 2000.

22. Silva, L.A.D. Desenvolvimento do Processo de Obtenção da Bentonita Organofílica de Moçambique: Síntese e Caracterização. Master's Thesis, Universidade Federal de Santa Catarina, Florianópolis, Brazil, 2013.

23. Macheca, A.; Gnanasekaran, D.; Focke, W.W. Surfactant-free dimer fatty acid polyamide/montmorillonite bio-nanocomposites. *Colloid Polym. Sci.* **2014**, *292*, 669–676.

24. Macheca, A.D.; Uwiragiye, B. Application of Nanotechnology in Oil and Gas Industry: Synthesis and Characterization of Organo-modified Bentonite from Boane Deposit and its Application in Produced Water Treatment. *Chem. Eng. Trans.* **2020**, *81*, 1081–1086.

25. Malai, A.S.; Macheca, A.D.; Cumbane, A.J. The Use of Mozambican Bentonite in Edible Oil Refining: Characterization, Acid Activation and Performance Evaluation. *Chem. Eng. Trans.* **2020**, *81*, 247–252.

26. Zhang, Y.; Jiang, T.; Chen, L.; Li, G. Study on sodium modification of inferior Ca-Based bentonite by suspension method. *Int. Sch. Res. Not.* **2011**, *2011*, 953132.

27. Lehto, T.; Gonçalves, R. Mineral resources potential in Mozambique. *Geol. Surv. Finl. Spec. Pap.* **2008**, *48*, 307–321.

28. Lopes, K.D.S. Avaliação da Etapa de Clarificação do óleo de soja Através de Planejamento Composto Central e Investigação do Potencial de Melhoria Energética no Processamento da Soja. Master's Thesis, Universidade Federal do Paraná, Curitiba, Brazil, 2008.

29. Nemukula, A.; Mutanda, T.; Wilhelmi, B.S.; Whiteley, C.G. Response surface methodology: Synthesis of short chain fructooligosaccharides with a fructosyltransferase from *Aspergillus aculeatus*. *Bioresour. Technol.* **2009**, *100*, 2040–2045. [PubMed]

30. Lee, K.E.; Morad, N.; Teng, T.T.; Poh, B.T. Evaluation of factors and kinetics study of polyacrylamide redox polymerization using statistical design modeling. *J. Polym. Eng.* **2012**, *32*, 215–224.

31. Calado, V.; Montgomery, D. *Planejamento de Experimentos Usando o Statistica*, 1st ed.; Editora E-Papers: Rio de Janeiro, Brazil, 2003; pp. 9–158.

32. Montgomery, D.C. *Montgomery Design and Analysis of Experiments*, 8th ed.; John Wiley & Sons, Inc.: Scottsdale, AZ, USA, 2013; pp. 65–553.

33. Chemtob, S.M.; Nickerson, R.D.; Morris, R.V.; Agresti, D.G.; Catalano, J.G. Synthesis and structural characterization of ferrous trioctahedral smectites: Implications for clay mineral genesis and detectability on Mars. *J. Geophys. Res.* **2015**, *120*, 1119–1140.

34. McLauchlin, A.R.; Thomas, N.L. Preparation and characterization of organoclays based on an amphoteric surfactant. *J. Colloid Interface Sci.* **2008**, *321*, 39–43.

35. Hassan, M.S.; Abdel-Khalek, N.A. Beneficiation and applications of an Egyptian bentonite. *Appl. Clay Sci.* **1998**, *13*, 99–115.

36. Odom, I.E. Smectite clay minerals: Properties and uses. *Philos. Trans. R. Soc. Land.* **1984**, *311*, 391–409.

37. Hong-Min, J. Effects of inorganic salt and temperature on the micro-structure of hydrated montmorillonite. *Acta Petrol. Sin.* **1998**, *19*, 122–127.